



## Liquid Metal Diagnostics

M. G. Hvasta, G. Bruhaug, A. E. Fisher, D. Dudt & E. Kolemen

To cite this article: M. G. Hvasta, G. Bruhaug, A. E. Fisher, D. Dudt & E. Kolemen (2019): Liquid Metal Diagnostics, Fusion Science and Technology, DOI: [10.1080/15361055.2019.1661719](https://doi.org/10.1080/15361055.2019.1661719)

To link to this article: <https://doi.org/10.1080/15361055.2019.1661719>



Published online: 18 Nov 2019.



Submit your article to this journal [↗](#)



View related articles [↗](#)



View Crossmark data [↗](#)



# Liquid Metal Diagnostics

M. G. Hvasta,<sup>a</sup> G. Bruhaug,<sup>b</sup> A. E. Fisher,<sup>b</sup> D. Dudt,<sup>c</sup> and E. Kolemen<sup>c\*</sup>

<sup>a</sup>*Alkali Consulting LLC, Lawrenceville, New Jersey*

<sup>b</sup>*University of Rochester, Rochester, New York*

<sup>c</sup>*Princeton University, Princeton, New Jersey*

Received June 16, 2018

Accepted for Publication August 16, 2019

**Abstract** — *Liquid metal (LM) plasma-facing components (PFCs) (LM-PFCs) within next-generation fusion reactors are expected to enhance plasma confinement, facilitate tritium breeding, improve reactor thermal efficiency, and withstand large heat and particle fluxes better than solid components made from tungsten, molybdenum, or graphite. Some LM divertor concepts intended for long-pulse operation at  $>20 \text{ MW/m}^2$  incorporate thin ( $\sim 1 \text{ cm}$ ), fast-moving ( $\sim 5$  to  $10 \text{ m/s}$ ), free-surface flows. Such systems will require a range of diagnostics to monitor and control the velocity, flow depth, temperature, and impurity concentration of the LM. This paper will highlight technologies developed for the fission and casting/metallurgical industries that can be adapted to meet the needs of LM-PFC research. This paper is divided into four major parts. The first part will look at noncontact flowmeter technologies that are suitable for high-temperature alkali metal systems. These technologies include rotating Lorentz-force flowmeters for bulk flow rate measurements and particle tracking techniques for surface velocity measurements. Second, this paper will detail the operation of a new inductive level sensor that can be used within free-surface LM-PFCs. This robust level sensor can be mounted below the substrate that supports the LM, so it is simple to install and is protected from the damaging conditions inside a fusion reactor. It has been shown that this level sensor can be calibrated using either numerical or experimental techniques. Third, distributed temperature sensors based on fiber-optic technologies will be discussed. This advanced measurement technique provides temperature data with high spatial resolution and has recently been successfully tested in LM systems. Last, diagnostics to measure impurity concentration, such as electrochemical cells, plugging meters, and spectroscopic systems, will be addressed.*

**Keywords** — *Liquid metal, flowmeter, impurity, level sensor, diagnostics.*

**Note** — *Some figures may be in color only in the electronic version.*

## I. INTRODUCTION AND BACKGROUND

Research and engineering efforts focused on liquid metal (LM) technologies for fission power plants started in the 1940–1950s. Liquid metals such as Na, NaK, Pb, and PbBi have been studied as heat transfer fluids within LM-cooled reactors due to their excellent thermal characteristics, high operating temperatures, low vapor pressures, and desirable neutronic properties.<sup>1,2</sup> Comparable research efforts for LM systems related to

fusion power began during the 1970s with a focus on Li, PbLi, Sn, and SnLi (3 through 6).

Because of the similarities between these two fields, many LM technologies originally developed for fission applications can be modified for fusion research. For example, engineers designing LM plasma-facing components (PFCs) (LM-PFCs) for next-generation fusion reactors can leverage preexisting tools and methods (e.g., piping fabrication techniques, electromagnetic pumps and flowmeters, impurity detection/removal devices, etc.) to handle large quantities of molten, high-temperature alkali metal. However, many new technologies must also be

---

\*E-mail: [ekolemen@princeton.edu](mailto:ekolemen@princeton.edu)

developed or adopted to address significant issues that are specific to LM-PFCs, namely,

1. detection and removal of tritium, impurities, and corrosion products from lithium systems
2. transient LM temperature measurements for pulsed, nonuniform power profiles within a reactor
3. characterization and control of free-surface, LM flows.

This paper will highlight key LM technologies from the fission and casting/metallurgical industries that can be directly translated to fusion research. Recent advances in LM diagnostics relevant to LM divertor operation will also be described. The first part of this paper will look at noncontact flowmeter technologies that are suitable for high-temperature alkali metal systems. Second, this paper will detail the operation of new inductive level sensors that can be used for free-surface LM-PFCs. Third, distributed temperature sensors utilizing fiber-optic systems will be discussed. The final section will address diagnostics that measure LM impurity concentration.

## II. NONCONTACT FLOWMETERS

As previous work has calculated,<sup>7</sup> a fusion power plant will require approximately 1.2 kg/s (2.4 L/s) of flowing lithium to remove 1 MW(thermal) from a reactor. Accurately and reliably measuring large flow rates throughout the reactor and the associated piping network will be a vital aspect of successful plant operation. Unfortunately, this task will be complicated by high operating temperatures, material compatibility issues, safety concerns over leakage and/or tritium containment, and challenges associated with installation and calibration. Accordingly, different flowmeter types will likely be required to handle the challenges unique to different components or systems within a fusion power plant. This section will briefly describe two different flowmeters. The first flowmeter could be used on pipes or tubes external to a fusion reactor to measure average LM velocities. The second flowmeter is capable of optically measuring the surface velocity of free-surface LM flows within the reactor.

### II.A. Rotating Lorentz-Force Flowmeters

Electromagnetic flowmeters have been used in high-temperature, alkali metal systems since the 1940s (8, 9, and 10). In general, electromagnetic flowmeters operate by

exposing electrically conductive fluids to a prescribed magnetic field and then correlating changes in localized voltage or flux density measurements to fluid velocity. Electromagnetic flowmeters are desirable in high-temperature alkali metal systems for two reasons. First, most electromagnetic flowmeters have no moving parts or seals in contact with the LM, which greatly reduces the risk of leakage and minimizes material compatibility issues. Second, many electromagnetic flowmeters can be installed external to a LM piping system, so there is typically no need to breach containment or risk contamination.

Rotating Lorentz-force flowmeters (RLFFs) are a unique type of electromagnetic flowmeter consisting of a circular array of permanent magnets that can spin upon a central, low-friction bearing. When this disk is placed next to a pipe filled with a flowing LM, the Lorentz force resulting from the relative motion between the magnet and the LM causes the flowmeter to rotate. The angular velocity of the rotating disk can then be correlated to the average velocity of the LM. This type of flowmeter was originally pioneered by Shercliff in 1957 (11) and 1960 (12) but has recently seen renewed interest in the past several years.<sup>13–17</sup> RLFFs could be a useful diagnostic for future LM systems within fusion power plants because they are inexpensive to produce and simple to install.

### II.B. Particle Tracking Flowmeters

The velocity of free-surface LM flows within a reactor can be challenging to measure because the flows are not contained within a pipe or tube and the flow depth and velocity profile may not be easily controlled.<sup>7,18</sup> Optical techniques for lithium<sup>19</sup> and galinstan<sup>20</sup> have been developed to measure the surface velocity using particle tracking techniques. Surface impurities were used as tracer particles in both of the referenced studies. The matte appearance of oxides and other impurities contrasts sharply with the highly reflective surface of most LMs. Similarly, differences in emissivity between LMs and impurities allow this technique to be used with infrared cameras.

One major limitation of the particle tracking technique is that cameras or other recording devices will likely need line-of-sight access to the LM-PFC. Another shortcoming of this method is that only surface velocities can be measured in opaque LMs. However, if the geometry of the LM-PFC and the flow parameters (e.g., depth, mass flow rate, etc.) are well known, it is possible that complete velocity profiles for free-surface flows could be calculated from known boundary conditions.

### III. LEVEL SENSORS

A variety of well-established level sensor designs and measurement techniques can be used to determine the depth or level of LM in a closed-loop system.<sup>1,21</sup> Typically, level sensors are placed in expansion tanks or dump tanks, which are large compared to the connected piping system, so that gradual changes in level can be tracked under quasi-static conditions. The most commonly used LM level sensors operate by (a) measuring the pressure differential between the bottom of a tank and the gas space above the LM, (b) tracking the location of thermal gradients, or (c) using an array of electrical probes. Unfortunately, most of the traditional methods require invasive instrumentation to be submerged into a LM, which could disrupt the fast-flowing surfaces found within LM-PFCs.

Under certain conditions, laser sheet diagnostics can be used to measure the depth of free-surface LM flows relevant to the casting industry<sup>22</sup> and fusion applications.<sup>18,23,24</sup> This noncontact level-sensing technique optically tracks changes in the location of a laser sheet impinging upon the surface of a LM to determine changes in depth without causing any surface waves or flow disturbances. However, like the particle tracking flowmeter described in Sec. II, this diagnostic requires line-of-sight access to the LM. Additionally, the performance of the laser sheet level sensor can be strongly affected by the presence (or absence) of matte oxides or other impurities on the surface of the LM that promote diffuse reflection.

#### III.A. Inductive Level Sensor

The aforementioned shortcomings of different LM-PFC level sensors can be largely addressed by using the noncontact, inductive level sensor depicted in Fig. 1. This noninvasive level sensor can be installed underneath or behind the substrate that supports the LM, which protects the level sensor from direct exposure to high-temperatures, corrosive LMs, and damaging plasma interactions. The solenoid within the level sensor is energized by an alternating-current power supply with constant peak-to-peak voltage. During operation, variations in LM thickness change the inductance of the circuit in a predictable way that can be numerically or experimentally calibrated (see Sec. III.C). The magnitude of the inductance change depends upon on the conductivity of the LM and the geometry of the system.

#### III.B. Inductive Level Sensor Theory

The measured inductance of the circuit  $L$  is affected by the presence of an electrically conductive LM. Under isothermal or steady-state conditions, the electrical resistivity of the LM and substrate will remain constant, so only changes in LM depth should affect the inductance of the circuit.

The level sensor shown in Fig. 1 can be analyzed as a simple resistor-inductor circuit (RL-circuit). For this analysis, assume the function generator provides a sinusoidal output with constant peak-to-peak voltage. The frequency  $f$  of the function generator can be adjusted or optimized as needed (see Sec. III.B.1). The magnitude of the current in the circuit  $I$  can be calculated with Eq. (1):

$$I = \frac{\Delta V_R}{R_R}, \quad (1)$$

where  $R_R$  is the known resistance of the shunt resistor and  $\Delta V_R$  is the measured peak-to-peak value of the voltage drop across the resistor. As depicted in Fig. 1, the value of  $\Delta V_R$  can be experimentally determined by using the oscilloscope to measure the voltage difference between Channel 1 and Channel 2.

The voltage across the solenoid  $\Delta V_L$  can be measured using Channel 2 of the oscilloscope. Using Eq. (2), one can calculate  $\Delta V_L$ :

$$\Delta V_L = IZ_L, \quad (2)$$

where  $Z$  is the impedance of the solenoid. More specifically,

$$Z_L = \sqrt{R_L^2 + X_L^2}$$

and

$$Z_L = \sqrt{R_L^2 + (2\pi fL)^2}, \quad (3)$$

where  $X_L$  is the inductive reactance of the solenoid and  $R_L$  is the resistance of the nonideal windings in the solenoid. After some algebraic manipulation, it can be shown that the inductance of the solenoid  $L$  can be calculated as

$$L = \frac{\sqrt{\left(\frac{R_R \Delta V_L}{\Delta V_R}\right)^2 - R_L^2}}{2\pi f}. \quad (4)$$

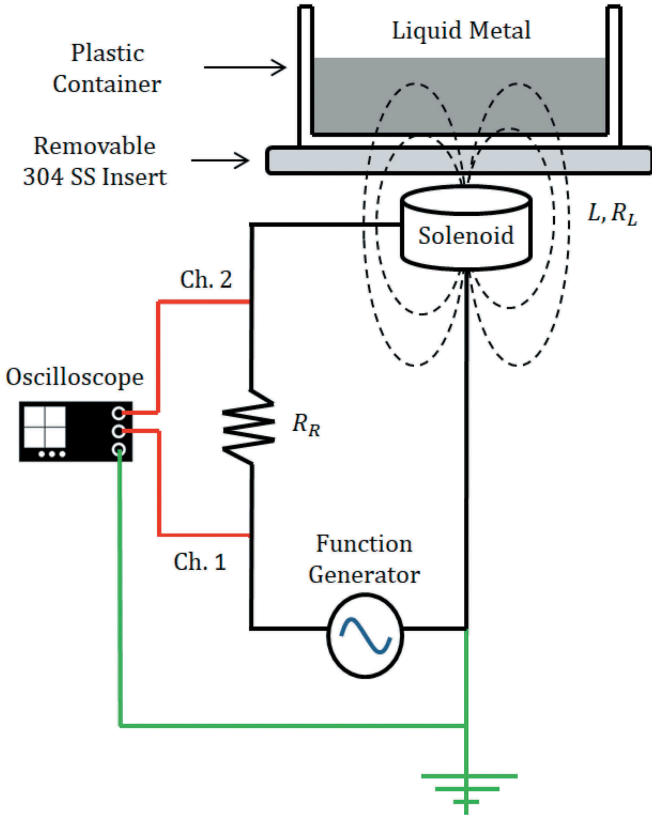


Fig. 1. A depiction of the noncontact inductive level sensor. All oscilloscope readings are referenced to ground. The resistor has resistance  $R_R$ . The nonideal solenoid has both resistance  $R_L$  and inductance  $L$ . The function generator produces a sinusoidal output with a constant peak-to-peak voltage.

During operation, changes to the inductance of the level sensor circuit can be attributed to changes of the LM thickness or level. If the properties of the LM are well known, the expected changes in inductance can be calculated using numerical techniques. If the properties of the liquid are not known, the inductive level sensor can be calibrated using other experimental techniques.<sup>20,21</sup>

### III.B.1. Inductive Level Sensor Operating Frequency

An appropriate level sensor operating frequency should be chosen such that the expected skin depth  $\delta_s$  is larger than any anticipated LM thickness. Skin depth, which is a measure of how far induced eddy currents penetrate into a conductor, can be approximated with Eq. (5):

$$\delta_s \approx \sqrt{\frac{\rho_e}{\pi f \mu_0 \mu_r}}, \quad (5)$$

where

$\rho_e$  = electrical resistivity of the LM

$\mu_0$  = vacuum permeability constant ( $4\pi \times 10^{-7}$  H/m)

$\mu_r$  = relative permeability of the LM.

The operating frequency of the level sensor must be appropriately selected for a given system. At low frequencies, changes to level sensor output may be too small to detect or too sensitive to background noise. At high frequencies, the time-varying signal may not penetrate the full depth of the LM. When LM depths are much greater than the skin depth, increasing LM thickness may not appreciably affect the output of the level sensor.

### III.C. Numerical Calibration and Experimental Results

The solenoid, LM, and substrate depicted in Fig. 1 can be modeled using an open-source finite element analysis software package known as Finite Element Magnetic Methods<sup>23</sup> (FEMM). An example of the axisymmetric FEMM model and output can be seen in Fig. 2. The Dirichlet boundaries can be seen forming a hemisphere around the entire model. The large multifaceted rectangle in the center of the picture represents regions of ‘‘Galinstan,’’ which is an alloy made from Ga-In-Sn that is liquid at room temperature. The off-center rectangle represents an axisymmetric cross section of the solenoid, and the lines emanating from the center of the picture represent the magnetic field lines.

In brief, the experimental setup consisted of a Wavetek 164 function generator that was configured to output a sinusoidal signal at 500 Hz. A Tektronix TDS-2004B oscilloscope was used to collect and analyze voltage measurements. The shunt resistor had a measured resistance of  $R_R = 2.772 \pm 0.003 \Omega$ . The hand-wound solenoid consisted of approximately 394 wraps of 24 AWG wire. The coil had an outer radius of  $2.76 \pm 0.025$  cm, an inner radius of  $1.40 \pm 0.025$  cm, a height of  $1.50 \pm 0.025$  cm, and a measured resistance of  $R_L = 4.779 \pm 0.004 \Omega$ .

The prototype level sensor was used to measure various galinstan depths contained within a thin-walled plastic container, and a comparison of the experimental and numerical results can be seen in Fig. 3. The inductance of the circuit was experimentally determined to be  $5.41 \pm 1.54 \times 10^{-2}$  mH when there was no galinstan in the container. As expected, the sensitivity of the level sensor began to decrease near the calculated skin depth of approximately 1.2 cm.

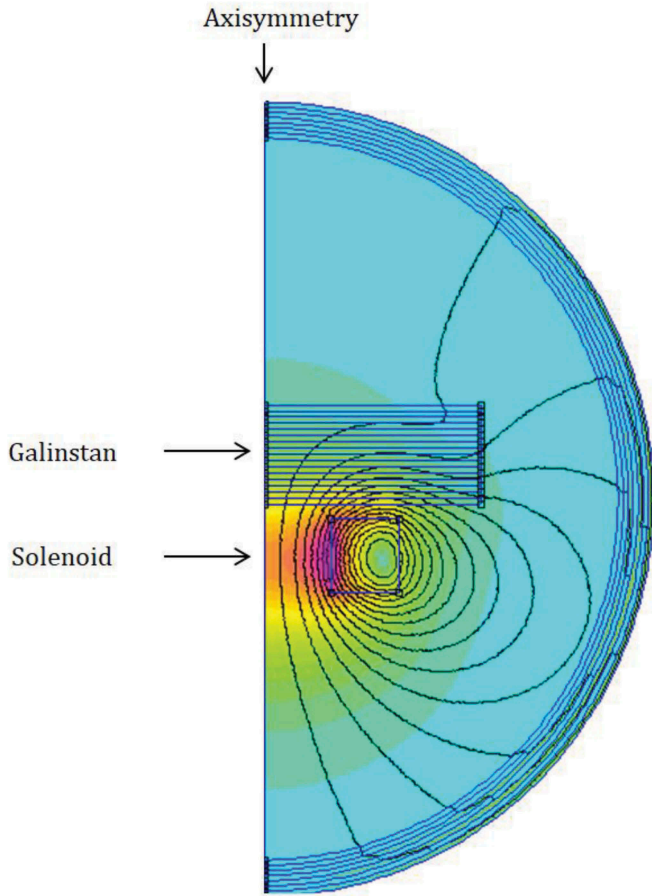


Fig. 2. FEMM output with 2 cm of galinstan. The magnetic field lines generated by the solenoid can be seen penetrating the galinstan.

#### IV. DISTRIBUTED TEMPERATURE MEASUREMENTS

Measuring transient, spatially dependent temperature profiles within free-surface LMs is an important aspect to successful LM-PFC operation. For example, without knowledge of real-time temperature profiles within flowing LMs, it may be difficult to calculate LM evaporation rates, power extraction, or local corrosion/deposition rates within a fusion reactor. Single-point temperature measurements using thermocouples or similar thermal sensors provide only limited insight into the thermal behavior of an LM-PFC. This limitation could be partially addressed by using infrared temperature measurements to image the entire surface of the LM. However, infrared diagnostics can measure only surface temperatures and will likely require line-of-site access to the LM-PFC, and measurements can be challenging due to the high reflectivity<sup>25</sup> and low emissivity<sup>26</sup> of the many LMs.

A promising new temperature-measuring technique using glass optical fibers has recently been adopted by LM researchers. The distributed temperature sensor consists of a single fiber-optic strand within a thin-walled stainless steel sheath that can be installed onto components or strung across LM-filled regions of interest. Slight density variations within the glass provide a Rayleigh backscatter profile that is locally stretched or compressed when the fiber is exposed to changing temperature profiles. When the glass fiber is connected

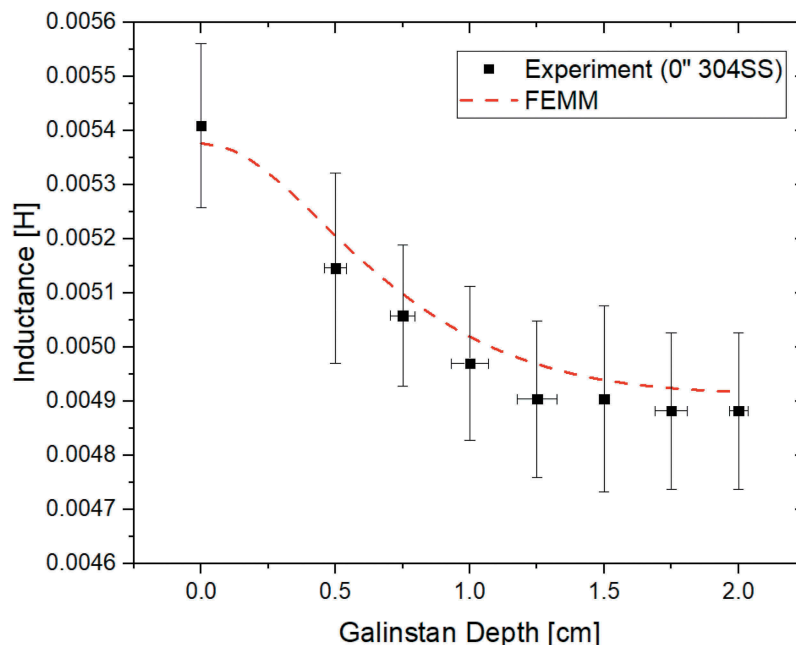


Fig. 3. Inductance of the level sensor versus galinstan height in a plastic (electrically insulating) container.

to a tunable laser and an interrogator circuit, the measured shift of the backscatter frequency can be used to calculate the semicontinuous temperature profile along the fiber.

To date, this temperature sensor has been used to study thermal stripping in high-temperature sodium systems.<sup>27</sup> It has also been used to study gas temperature profiles<sup>28</sup> and the gas-liquid interface in high-temperature molten salt systems.<sup>29</sup> This technology has the potential to provide high-resolution thermal data for LM-PFCs. In turn, it is possible that high-fidelity experimental data collected using this technique could be used to benchmark computational fluid dynamics/magnetohydrodynamics codes for next-generation fusion systems.

## V. IMPURITY DETECTION

Similar to LM-cooled fast fission reactors, LM-PFC systems will need to mitigate impurity and corrosion issues due to interactions between high-temperature LMs and the piping systems and/or substrates. Moreover, LM-PFCs must also be able to accommodate extra impurity collected by the LM within the reactor due to intentional gas and fuel injections. Accurately measuring and subsequently controlling impurity levels within LM-PFCs has been identified as a major need for fusion-related LM research.<sup>30</sup> Beyond being able to detect and control tritium concentrations within LM systems, next-generation fusion power plants must be able to measure and limit oxygen or other impurities that could cause unwanted plugging or accelerated corrosion.<sup>31,32</sup>

Devices such as plugging meters<sup>33</sup> are a robust and reliable tool for determining impurity levels within LMs. Plugging meters are commonly installed in small bypass loops connected to the main piping system. The device operates by cooling the LM flowing through it to temperatures near its freezing point where the solubility of impurities in the LM is reduced. If/when the LM becomes supersaturated, impurity will precipitate out of solution and adhere to a custom flow restriction. By monitoring LM temperature and reductions in flow rate through a plugging meter, the saturation temperature of impurities can be determined. Using experimental data or other correlations, the impurity concentration can then be calculated using the measured saturation temperature.<sup>34</sup> However, plugging meters are indiscriminate and generally cannot differentiate between different types of impurities. Additionally, for some fusion-relevant LMs like lithium, plugging meters may not be useful for low-level hydride detection since the saturation concentration

near freezing is  $\sim 400$  atomic parts per million (appm) (Ref. 35).

Electrochemical impurity sensors,<sup>36</sup> which are designed to specifically measure one impurity (e.g., oxygen), can supplement plugging meter measurements. However, in alkali metal systems, ceramic electrolytes can be hindered by material compatibility issues and limited mechanical integrity. Additionally, some electrochemical sensors have a very narrow temperature band in which they can operate, so they are not suitable for installation in all parts of the LM system.

Laser-induced breakdown spectroscopy (LIBS) is a promising technology that has recently been adapted to LM research in the casting/metallurgical industries.<sup>37,38</sup> As its name suggests, LIBS uses a laser to locally heat a small portion of the LM surface and generate a localized plasma. (For some applications it may be desirable to produce a similar excitation with an electric arc using a spark gap.) The spectra from this small plasma are then analyzed to determine the composition of the LM and concentration of impurities. Depending on the composition of the impurities within the LM, sensitivities in the range of  $\sim 1$  to 10 appm can be achieved.

This diagnostic would likely need to be installed into the gas space above the LM within a custom vessel. Proper purging and venting with an inert gas may need to be used to prevent LM vapor from collecting on the spectrometer or other sensitive diagnostics. However, despite these potential issues, this technology could be useful as an on-demand, in situ diagnostic within a fusion facility or as a means to calibrate other LM impurity sensors.

## VI. DISCUSSION

This paper has identified several technologies that can help address technical challenges facing the development of LM-PFCs for next-generation fusion reactors. Many of the diagnostics highlighted in this paper were originally developed for the fission and casting/metallurgical industries but could be readily adapted to LM-PFC research. Newer technologies, such as noncontact inductive level sensors, distributed temperature measurement systems, and spectroscopic impurity detection, were also discussed. It is hoped that advances in LM diagnostics will continue to be generated across multiple industries and fields of research in order to help make fusion power technically feasible and economically viable.

## Acknowledgments

The research described in this paper was conducted under the Laboratory Directed Research and Development Program at Princeton Plasma Physics Laboratory, a national laboratory operated by Princeton University for the U.S. Department of Energy under prime contract number DE-AC02-09CH11466. The digital data for this paper can be found at <http://arks.princeton.edu/ark:/88435/dsp01x920g025r>.

This manuscript is based upon work supported by the U.S. Department of Energy, Office of Science, Office of Fusion Energy Sciences, and has been authored by Princeton University under Contract Number DE-AC02-09CH11466 with the U.S. Department of Energy. The publisher, by accepting the article for publication acknowledges, that the United States Government retains a non-exclusive, paid-up, irrevocable, world-wide license to publish or reproduce the published form of this manuscript, or allow others to do so, for United States Government purposes.

## ORCID

M. G. Hvasta  <http://orcid.org/0000-0002-8934-711X>

G. Bruhaug  <http://orcid.org/0000-0002-0217-3146>

A. E. Fisher  <http://orcid.org/0000-0003-1744-6984>

D. Dudt  <http://orcid.org/0000-0002-4557-3529>

E. Kolemen  <http://orcid.org/0000-0003-4212-3247>

## References

1. R. N. LYON, *Liquid-Metals Handbook*, Atomic Energy Commission (1950).
2. “Liquid Metal Coolants for Fast Reactors Cooled by Sodium, Lead, and Lead-Bismuth Eutectic,” International Atomic Energy Agency (2012).
3. D. P. JACKSON, “A Review of Fusion Breeder Blanket Technology—Part 1/Review and Findings,” Canadian Fusion Fuels Technology Program (1985).
4. “Present Status of Liquid Metal Research for a Fusion Reactor,” *Plasma Phys. Control. Fusion*, **58**, 014014 (2016); <https://doi.org/10.1088/0741-3335/58/1/014014>.
5. M. A. ABDU et al., “Overview of Fusion Blanket R&D in the US over the Last Decade,” *Nucl. Eng. Technol.*, **37**, 401 (2005).
6. R. WOOLLEY, “Method and Apparatus to Produce and Maintain a Thick, Flowing, Liquid Lithium First Wall for Toroidal Magnetic Confinement DT Fusion Reactors”. U.S. Patent 6,411,666 (June 25, 2002).
7. M. G. HVASTA et al., “Demonstrating Electromagnetic Control of Free-Surface, Liquid-Metal Flows Relevant to Fusion Reactors,” *Nucl. Fusion*, **58**, 1 (2017).
8. J. A. SHERCLIFF, *The Theory of Electromagnetic Flow-Measurement*, Cambridge University Press (1962).
9. J. A. SHERCLIFF, “Steady Motion of Conducting Fluids in Pipes Under Transverse Magnetic Fields,” *Math. Proc. Cambridge Philos. Soc.*, **49**, 1, 136 (1953); <https://doi.org/10.1017/S0305004100028139>.
10. G. E. TURNER, “Liquid Metal Flow Measurement (Sodium) State-of-the-Art Study (LMEM-Memo-68-9),” Liquid Metal Engineering Center (1968).
11. J. A. SHERCLIFF, “Tests with Mercury of a Rotating Flowmeter for Liquid Metals,” United Kingdom Atomic Energy Authority (1957).
12. J. A. SHERCLIFF, “Improvements in or Relating to Electromagnetic Flowmeters.” Great Britain Patent GB831226 (Mar. 23, 1960).
13. I. BUCENIEKS, “Modelling of Induction Rotary Permanent Magnet Flowmeters for Liquid Metal Flow Control,” *Magneto hydrodynamics*, **50**, 157 (2014); <https://doi.org/10.22364/mhd.50.2.4>.
14. I. BUCENIEKS, “Experimental Measurements of Sensitivity of Cylindrical Rotary Induction Flowmeter on Permanent Magnets,” *Proc. 2nd Int. Workshop Measuring Techniques for Liquid Metal Flows*, Dresden, Germany, 2007.
15. M. G. HVASTA et al., “Experimental Calibration Procedures for Rotating Lorentz-Force Flowmeters,” *Meas. Sci. Technol.*, **28**, 8, 085901 (2017); <https://doi.org/10.1088/1361-6501/aa781b>.
16. M. G. HVASTA et al., “Calibrationless Rotating Lorentz-Force Flowmeters for Low Flow Rate Applications,” *Meas. Sci. Technol.*, **29**, 7 (2018).
17. M. RATAJCZAK et al., “Measurement Techniques for Liquid Metals,” *IOP Conf. Ser. Mater. Sci. Eng.*, **228**, 012023 (2017); <https://doi.org/10.1088/1757-899X/228/1/012023>.
18. A. E. FISHER, E. KOLEMEN, and M. G. HVASTA, “Experimental Demonstration of Hydraulic Jump Control in Liquid Metal Channel Flow Using Lorentz Force,” *Phys. Fluids*, **30**, 067104 (2018); <https://doi.org/10.1063/1.5026993>.
19. M. JAWORSKI et al., “Thermoelectric Magneto hydrodynamic Stirring of Liquid Metals,” *Phys. Rev. Lett.*, **104**, 094503 (2010); <https://doi.org/10.1103/PhysRevLett.104.012001>.
20. M. G. HVASTA, E. KOLEMEN, and A. E. FISHER, “Application of IR Imaging for Free-Surface Velocity Measurement in Liquid-Metal Systems,” *Rev. Sci. Instrum.*, **88**, 1, 013501 (2017); <https://doi.org/10.1063/1.4973421>.
21. H. W. SLOCOMB, “Liquid Metal Level Measurement (Sodium) State-of-the-Art-Study,” Liquid Metal Engineering Center (1967).
22. D. C. MEEKER, “Finite Element Method Magnetics – Version 4.2,” <http://www.femm.info> (current as of 2016).
23. M. NARULA, A. YING, and M. A. ABDU, “A Study of Liquid Metal Film Flow, Under Fusion Relevant Magnetic

- Fields,” *Fusion Sci. Technol.*, **47**, 564 (2005); <https://doi.org/10.13182/FST05-A745>.
24. M. S. NARULA, “Experiments and Numerical Modeling of Fast Flowing Liquid Metal Thin Films Under Spatially Varying Magnetic Field Conditions,” PhD Thesis, University of California, Los Angeles (2008).
  25. L. A. AKASHEV and V. I. KONONEKO, “Optical Properties of Liquid Gallium-Indium Alloy,” *Tech. Phys.*, **43**, 118 (1998); <https://doi.org/10.1134/1.1259083>.
  26. A. ARTHURS et al., “Measurement of the Emissivity of Liquid Gallium Alloy for Temperature Measurements of Free-Surface Flows,” *Proc. 52nd Annual Mtg. APS Division of Plasma Physics*, Chicago, Illinois, November 8–12, 2010, American Physical Society (2010).
  27. M. WEATHERED et al., “Characterization of Thermal Striping in Liquid Sodium with Optical Fiber Sensors,” *ASME J. Nucl. Rad. Sci.*, **3**, 4, 041003 (2017); <https://doi.org/10.1115/1.4037118>.
  28. S. LOMPERSKI, C. GERARADI, and D. LISOWSKI, “Fiber-Optic Distributed Sensors for High-Resolution Temperature Field Mapping,” *J. Vis. Exp.*, **117**, 54076 (2016).
  29. M. WEATHERED and M. ANDERSON, “On the Development of a Robust Optical Fiber-Based Level Sensor,” *IEEE Sens. J.*, **18**, 2, 583 (2018); <https://doi.org/10.1109/JSEN.2017.2777801>.
  30. “Fusion Energy Sciences Advisory Committee Report: Transformative Enabling Capabilities for Efficient Advance Toward Fusion Energy,” U.S. Department of Energy Office of Fusion Energy Sciences (2018).
  31. H. KATSUTA and K. FURUKAWA, “Air Contamination Effects on the Compatibility of Liquid Lithium with Molybdenum, TZM, Niobium, Stainless Steel, Nickel, and Hastelloy N in Stainless-Steel Vessels at 600°C,” *J. Nucl. Mater.*, **71**, 94 (1977); [https://doi.org/10.1016/0022-3115\(77\)90192-1](https://doi.org/10.1016/0022-3115(77)90192-1).
  32. B. MISHRA and D. L. OLSON, “Corrosion of Refractory Alloys in Molten Lithium and Lithium Chloride,” *Miner. Process. Extr. Metall. Rev.*, **22**, 369 (2002); <https://doi.org/10.1080/08827500208547421>.
  33. C. C. MCPHEETERS and J. C. BIERY, “The Dynamic Characteristics of a Plugging Indicator for Sodium,” *Nucl. Appl.*, **6**, 6, 573 (1969); <https://doi.org/10.13182/NT69-A28287>.
  34. J. D. NODEN, “A General Equation for the Solubility of Oxygen in Liquid Sodium,” *J. Br. Nucl. Energy Soc.*, **12**, 1, 57 (1973).
  35. D. K. SZE et al., “Tritium Recovery from Lithium Based on Cold Trap,” Argonne National Laboratory (1994).
  36. B. K. NOLLET et al., “Development of an Electrochemical Oxygen Sensor for Liquid Sodium Using a Yttria Stabilized Zirconia Electrolyte,” *J. Electrochem. Soc.*, **164**, 2, B10 (2017); <https://doi.org/10.1149/2.0021702jes>.
  37. J. GRUBER et al., “Rapid In-Situ Analysis of Liquid Steel by Laser-Induced Breakdown Spectroscopy,” *Spectrochim. Acta B*, **56**, 6, 685 (2001); [https://doi.org/10.1016/S0584-8547\(01\)00182-3](https://doi.org/10.1016/S0584-8547(01)00182-3).
  38. S. W. HUDSON et al., “Applications of Laser-Induced Breakdown Spectroscopy (LIBS) in Molten Metal Processing,” *Metall. Mater. Trans. A Phys. Metall. Mater. Sci.*, **48**, 5, 2731 (2017); <https://doi.org/10.1007/s11663-017-1032-7>.